International Journal of Advanced Chemistry Research 2024; 6(2): 01-08

ISSN Print: 2664-6781
ISSN Online: 2664-679X
IJACR 2024; 6(2): 01-08
www.chemistryjournals.net
Received: 02-05-2024
Accepted: 07-06-2024

Walaa Hazim Hameed
Tikrit University, Salahuddin, Iraq

Nashwan Hussein Ali
Samara University, Salahuddin, Iraq

Corresponding Author:
Walaa Hazim Hameed
Tikrit University, Salahuddin, Iraq

Synthesis and characterization of Alginate-Ag-attapulgite with different ratios of hydroxyapatite nanoparticles

Walaa Hazim Hameed and Nashwan Hussein Ali

DOI: https://doi.org/10.33545/26646781.2024.v6.i2a.203

Abstract
In order to enable the in situ bio reduction of Ag ions, our work involves the ecologically friendly creation of a brown attapulgite-Ag nanocomposite using bay leaf extract. This enables good stability and dispersion of Ag NPs together with an effective enhancement in activity and biofriendliness. In order to improve the performance of the alginate-attaplugite-AgNps nanocomposite as an advanced adsorbent material, three different weights (0.1, 0.2, and 0.4 g) of hydroxyapatite nanocomposite were added. The resultant nanocomposite was characterized using XRD, SEM, BET, and TEM. As a result, given its higher bio-performance and cleaner, ecologically friendly production process, the created alginate-attaplugite-AgNps nanocomposite may have significant potential usage in a range of domains, such as food preservation, wound care, and antibacterial or as adsorbent materials.

Keywords: Synthsis, characterization, alginate-attapulgite-AgNps

Introduction
Alginates have been created and applied all over the world for a very long period. In the latter half of the 1800s, British scientist E.C.C. Stanford made the first known discovery of alginates. Since then, a lot of research has been done on alginates to discover more about their properties and potential applications. The popularity of alginate, a biopolymer found in sea algae, has increased mostly composed of linear polymers of β-(1-4)-D-mannuronic (M) and α-L-gluronic (G) acids, which have different linear configurations and ratios [1, 2]. Alginate's massive molecular mass gives it a high viscosity and gel strength [3]. Alginate's high molecular weight contributes to its poor solubility and bioavailability [4-5]. Alginates' remarkable properties with regard to renewability, biocompatibility, biodegradation, and processing have led to their widespread usage and investigation in a variety of fields, including tissue engineering, medication delivery, wound healing, textile, cosmetics, and food science. In industrial food processing, alginates are commonly utilized as coating compounds that resist microorganisms and as thickeners and stabilizers [6]. Because of its biodegradability, it is the ideal raw material for active packaging films used in the food and pharmaceutical industries [7]. Furthermore, the use of alginates and their composites in electrode modification has been the subject of some research [8], the removal of contaminants [9], and the fermentation of dormant cells [10].
Pure alginate salts unquestionably have a poorly formed structure [11]. Because these properties are directly related to their capacity to function as encapsulating materials, alginates are commonly identified by their average molecular weight and M/G ratio [12]. Alginates are often extracted and purified by first changing from an insoluble to a soluble state within the algal cell walls, typically with the aid of sodium salt. Then, a sequence of precipitations and dissolutions is carried out to eliminate any leftover pollutants [13]. Because of their many uses, nanocomposites are now thought to be extremely important materials [14-18]. Since they are inexpensive and simple to produce in large quantities for industrial use, the nanostructured clays containing metal nanoparticles or metal oxide nanoparticles are the most significant of these composites [19-21].

A kind of hydrated magnesium aluminium silicate mineral called attapulgite (ATP) is made up of magnesium organized in an octahedral coordination and silicon dioxide shaped like a tetrahedron. The structural formula (OH2)4(Mg, Al, Fe)5(OH) is used to represent it. The oxygen atoms (2Si8O20) that the attapulgite units share bind the units together. The channels run the length of the crystals because of the partially organized water, which creates borders that resemble ribbons. The Mg (Al, Fe) brucite's magnesium cations are linked to the partially ordered water. Attapulgite creates a lattice structure of particles linked by hydrogen bonds that causes gel formations in both fresh and saline water. Among its many benefits are its excellent mechanical and thermal stability, affordability, accessibility, and lack of toxicity [22].

Because of its biological characteristics, silver nanoparticles differ from other metal nanoparticles. Silver nanoparticles have been shown in numerous studies to possess significant biological capabilities, including antimicrobial, antiviral, wound-healing, and anti-inflammatory effects [23-25]. Metallic nanoparticles (NPs) are commonly prepared by conventional chemical and physical methods. However, modern environmental concerns have prompted research into green synthesis and eco-friendly synthesis in order to manufacture metallic NPs based on a range of biological entities [26]. This review does not aim to cover all plant extracts used in the green synthesis of AgNPs. Reviews [27-29] discuss this field in great detail. Rather, this review focuses primarily on the synthesis of AgNPs using plant extracts as reducing agents. Silver nanoparticles are commonly produced using a variety of sources, including bacteria, fungi, plants, and biopolymers. In this reaction, Ag + and the functional components of various plant extract constituents interact electrostatically [30]. Silver nanoparticles are particularly important for their chemical and biological characteristics, among other reasons. Unwanted byproducts are produced during synthesis due to the usage of hazardous components. As such, there is an increasing need to create environmentally benign processes for the green production of nanoparticles. Consequently, research into the ecologically benign synthesis of Ag-NPs is emerging as an important field of study in nanotechnology. Biological resources, such as microorganisms, plant extracts, or both, can be used in place of physical and chemical interactions to make environmentally acceptable NPs [31]. Hydroxyapatite (HAp), an inorganic substance with the chemical formula CA10 (PO4)6(OH)2, has received a lot of attention as a graft component due to its exceptional biocompatibility in the medical industry. It is widely used in several fields, including environmental conservation and dental restoration [32, 33]. HAp has been used recently in numerous biological processes, including wound healing, drug transport, and tissue engineering [34]. Scientists have determined that hydroxyapatite (HAP) is the best adsorbent material for removing and recovering contaminants from water [35]. HAP has been effectively utilised to remove a variety of contaminants from wastewater due to its exceptional surface characteristics. Review articles that were recently published discuss the use of HAP as a flexible material for environmental remediation [36, 37].

One of the aims of the study was to reduce the usage of Iraqi attapulgite clays, whose supply seems to have disappeared. This goal was successfully met because the study only requires small amounts of the material.

The synthetically produced composite materials exhibited encouraging adsorption properties. They seem to be promising adsorbents in the processes of removing organic pollutants. Furthermore, the alginate-attaplugite-AgNps composites' constituents are biodegradable and harmless for the environment.

Alginate has demonstrated chemical stability. The chemical has an excellent structure and significant adsorption properties, according to study analysis.

Materials and Methods

1. Preparation of bay leaf extract

The bay leaf was dried and sieved after being baked for three days at 40 to 45 degrees Celsius and ground into a fine powder using a combination grinder. Combine 10g of leaf powder and 100ml of deionized water in a 500ml flask. Boil for 10 to 15 minutes, then allow to come down to room temperature. After filtering the cooled mixture through Whatman filter paper number 1, collect the filtrate.

2. Ag NPs-attapulgite

After dissolving two grammes of AgNO3 in 150 millilitres of deionized water and heating to 60 degrees Celsius, 10 grammes of attapulgite clay were added to the mixture in order to equally distribute the silver ions throughout the clay. The mixture was then stirred for a further fifteen minutes. After that, bay leaf extract was added, bringing the total capacity up to roughly 250 ml. The mixture was stirred for an hour at room temperature, filtered, and rinsed three times with deionized water before being dried at 60 degrees Celsius for a duration of twelve hours.

3. Alginate gel

To make the alginate gel, two grammes of sodium alginate and one hundred millilitres of cold water were mixed together and shaken for a full day.

4. Alginate-Ag NPs-attapulgite-hydroxyapatite

Accompanying the alginate gel, a whole mixture of 100 ml and 1 g Ag NPs-attapulgite was utilized to produce matched composites with varying HA contents. Subsequently, 0.1, 0.2, and 0.4 g of hydroxyl apatite nanoparticles were added individually. After it was established that the combination was homogeneous, it was sonicated one more utilizing water bath ultrasonography equipment. The composite gel was then put into a beaker containing a gelation agent (One gramme dissolved in one hundred millilitres). After being collected, the droplet was cleaned with distilled water, dried for half an hour at 60 degrees Celsius, and then utilized again in the subsequent steps.

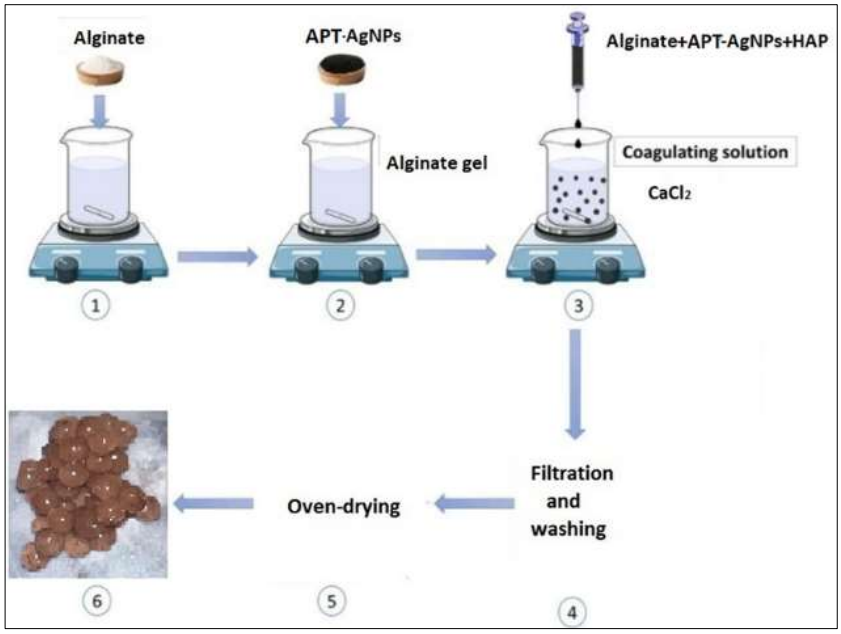

Fig 1: Preparation of Alg-APT-AgNPs Nanocomposite

Results and discussion

Characterization of nanocomposites

Characterization of Ag-attapulgite nanocomposite

XRD

The observations in Figure 2 demonstrated the presence of the distinctive attapulgite peaks at 19.943, 29.293, 37.193, and 45.093°, respectively, which correspond to montmorillonite, calcite, and palygorskite. Using this parameter, the reaction's efficacy was evaluated. The usual nanosilver peaks at 46.293, 67.793, 76.943°, and 37.193° were also seen in the measurement. These peaks correspond to the crystal planes of 111, 200, 220, and 311, respectively, and are related to the creation of the nanosilver facing centre cubic crystal system. The measurement thus demonstrates the efficacy of the attapulgite and nanosilver interaction, but it also reveals that the low-crystallinity clay decreased the silver's crystallinity (38, 39). As indicated in Table 1, the crystalline size was estimated using the Scherrer equation. The findings indicated that the average particle size was 50.98 nanometers, with a range of about 2-146 nanometers

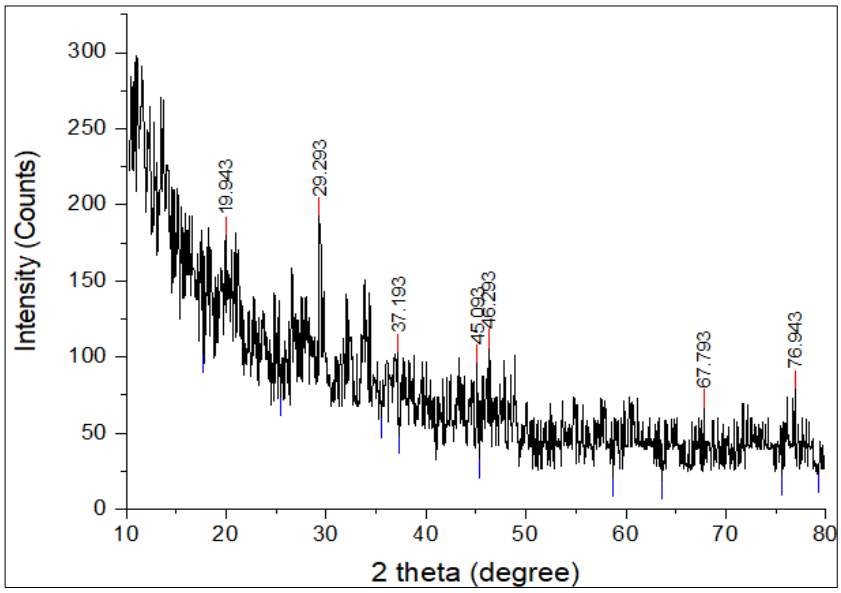

Fig 2: XRD of Ag-attapulgite nanocomposite

Table 1: XRD data of Ag -attapulgite nanocomposite

Position (o)	FWHM (o)	Particle size (nm)	Average particle size (nm)	Assignment
19.943	3.93167	2.14	50.98	Montomorillonite
29.293	0.33651	25.50		Calcite
37.193	0.99306	8.82		Ag NPs and Palygorskite
45.093	0.17	52.89		Palygorskite
46.293	0.13977	64.61		Ag NPs
67.793	0.06827	146.53		Ag NPs
76.943	0.18813	56.38		Ag NPs

SEM: For the purpose of characterising nanomaterials, particularly those with well-known nanostructures like attapulgite, this measurement is thought to be crucial. Figure 3 measurement revealed geometric patterns that looked like different channels stacked on top of one another; these characteristics are thought to be unique to attapulgite. The measurement provides more evidence of the response between the attapulgite and the nanosilver. It also demonstrates how the nanosilver ornamentation formed rough surfaces on the attapulgite surfaces as the silver sintered on the attapulgite surface. The measurement showed the attapulgite containing nanosilver to have a diameter of less than 47 nanometers, which is consistent with the Scherrer equation-derived estimated particle size of 50.98 nm from X-ray diffraction.

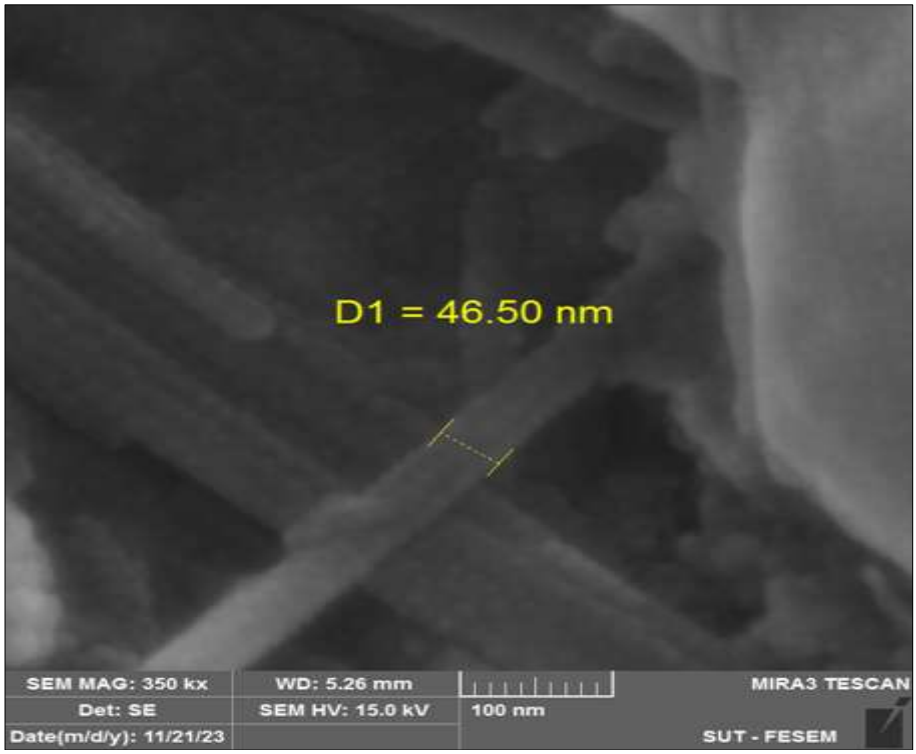

Fig 3: SEM of Ag -attapulgite nanocomposite

Characterization of alginate-Ag -attapulgite-hydroxyapatite nanocomposite

XRD

Figure 4's XRD measurement revealed the distinctive alginate peaks at 14.793 and 25.943° (40), whereas calcite and palygorskite were identified as the source of the attapulgite peaks (28.893, 38.143, and 42.043°). Additionally, hydroxyapatite was detected at 28.893, 31.693, 32.743, 34.193, 40.043, 49.243, 52.943, and 63.693°. These coordinates are assigned to the crystal planes 210, 211, 112, 202, 130, 213, 321, and 084, in that order. Ultimately, for the facing cubic centre, the measurement revealed the distinct nanosilver peaks at 38.143, 46.743, 63.693, and 74.943°. The Scherrer equation is employed in Table 2 to get the average particle size, which was found to be 10.52 nm.

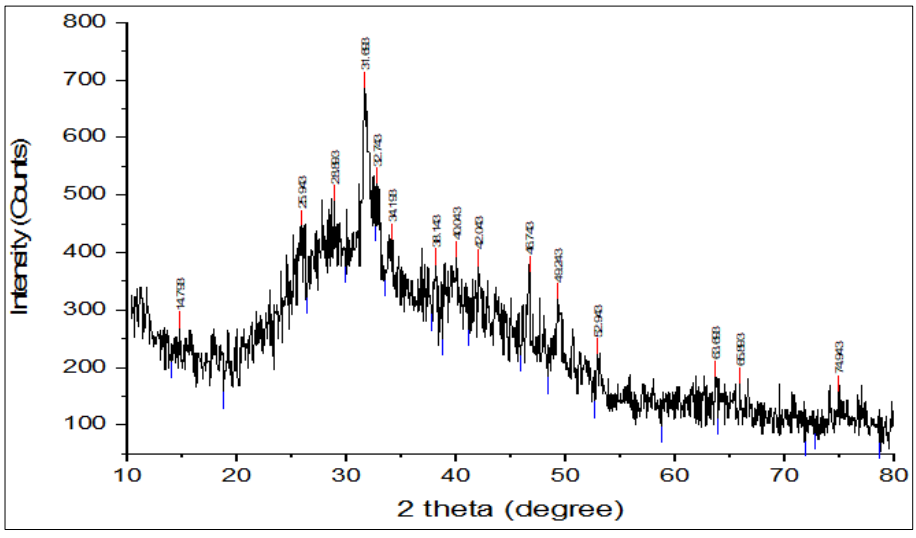

Fig 4: XRD of alginate-Ag -attapulgite-hydroxyapatite nanocomposite

Table 2: XRD data of alginate-Ag -attapulgite-hydroxyapatite

Position (o)	FWHM (o)	Particle size (nm)	Average particle size (nm)	Assignment
14.793	2.29881	3.64	10.52	Alginate
25.943	2.14079	3.98		Alginate
28.893	3.55	2.42		Calcite and Hydroxyapatite
31.693	1.39896	6.17		Hydroxyapatite
32.743	0.75	11.54		Hydroxyapatite
34.193	4.25	2.04		Hydroxyapatite
38.143	0.9	9.76		Ag NPs and Palygorskite
40.043	2.35	3.76		Hydroxyapatite
42.043	3.64891	2.44		Palygorskite
46.743	1.13387	7.98		Ag NPs
49.243	1.81393	5.04		Hydroxyapatite
52.943	1.09751	8.45		Hydroxyapatite
63.693	0.36724	26.62		Ag NPs
65.893	0.31944	30.98		Ag NPs
74.943	0.3174	32.96		Ag NPs

SEM

Alginate balls containing attapulgite, silver, and hydroxyapatite were used for this measurement. This measurement's findings showed a smooth surface with many aggregate structures, which are assumed to be the product of the composite particles inside the ball. The measurement also confirmed the presence of channel-like structures assigned to the attapulgite and irregular and spherical particles attributed to the other components in the attapulgite-silver-hydroxyapatite composite. These results show that the polymeric combination for the composite, as shown in Figure 5, is successful.

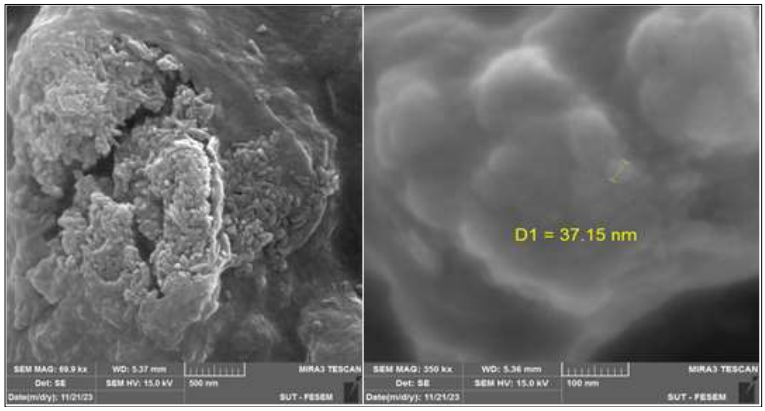

Fig 5: SEM of alginate-Ag -attapulgite-hydroxyapatite nanocomposite

TEM: As seen in Figure 6, the measurement revealed the presence of unique structures of nanosilver (as nanospheres), hydroxyapatite (as irregular structures), and attapulgite (as individual nanorods). The diameter of the attapulgite was measured and found to be 6-20 nanometers, the diameter of the hydroxyapatite was found to be no more than 60 nanometers, and the diameter of the silver was found to be 10-30 nanometers.

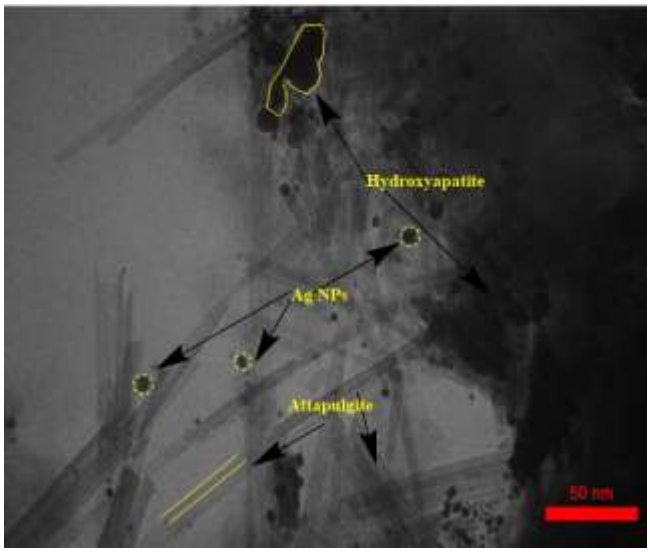

Fig 6: TEM of alginate-Ag -attapulgite-hydroxyapatite nanocomposite

BET: The measurement demonstrated the existence of distinct nanosilver (as nanospheres), hydroxyapatite (as irregular structures), and attapulgite (as individual nanorods) structures, as shown in Figure 6. The measurements revealed that the attapulgite had a diameter of 6-20 nanometers, the hydroxyapatite had a diameter of no more than 60 nanometers, and the silver had a diameter of 10-30 nanometers.

Table 3: Surface area results of alginate-Ag -attapulgite-hydroxyapatite

BET plot		
V_m	5.0702	[cm^3(STP) g^{-1}]
$a_{s,BET}$	122.068	[m^2 g^{-1}]
C	82.114	
Total pore volume(p/p_0=0.990)	0.1061	[cm^3 g^{-1}]
Average pore diameter	19.234	[nm]
Langmuir plot		
V_m	5.629	[cm^3(STP) g^{-1}]
$a_{s,Lang}$	124.5	[m^2 g^{-1}]
B	0.9057	
t plot		
Plot data	**Adsorption branch**	
a_1	118.643	[m^2 g^{-1}]
V_1	0	[cm^3 g^{-1}]
a_2	154.228	[m^2 g^{-1}]
V_2	-0.024909	[cm^3 g^{-1}]
2t	1.3914	[nm]
BJH plot		
Plot data	**Adsorption branch**	
V_p	0.1093	[cm^3 g^{-1}]
$r_{p,peak}$(*Area*)	6.95	[nm]
a_p	127.375	[m^2 g^{-1}]

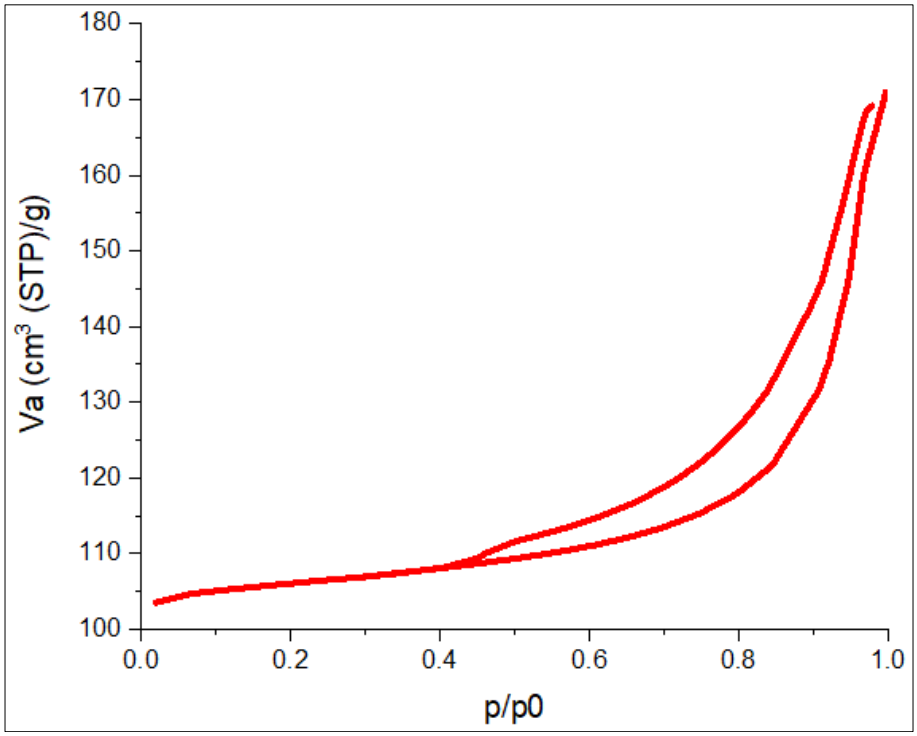

Fig 7: BET of alginate-Ag -attapulgite-hydroxyapatite nanocomposite

Conclusion

Based on the results of this study, we can use attapulgite impregnated with nanoscale silver in an environmentally friendly way by using extract from bay leaves as a reducing agent. This suggests that the addition of APT significantly decreased the size of Ag NPs and enhanced their dispersion. Therefore, in addition to having outstanding bio-performance, the alginate-attaplugite-AgNps nanocomposite that was created in this study offers the benefits of being simple, affordable, and ecologically benign. It may therefore find utility as a nanomaterial in numerous industries, such as wound healing, food preservation, and antimicrobial and medicinal applications.

References

1. Kokilam G, Vasuki S, Sajitha N. Biochemical composition, alginic acid yield and antioxidant activity of brown seaweeds from Mandapam region, Gulf of Mannar. J Appl. Pharm Sci. 2013;3(11):99-104.

2. Sharma A, Gupta MN. Three phase partitioning of carbohydrate polymers: Separation and purification of alginates. Carbohydr Polym. 2002;48(4):391-395.
3. Yoon HJ, Hashimoto W, Miyake O, Okamoto M, Mikami B, Murata K, *et al*. Overexpression in *Escherichia coli*, purification, and characterization of *Sphingomonas* sp. A1 alginate lyases. Protein Expr. Purif. 2000;19(1):84-90.
4. Murata K, Inose T, Hisano T, Abe S, Yonemoto Y, Yamashita T, *et al*. Bacterial alginate lyase: enzymology, genetics and application. J Ferment Bioeng. 1993;76(5):427-437.
5. Wang B, Dong S, Li FL, Ma XQ. Structural basis for the exolytic activity of polysaccharide lyase family 6 alginate lyase BcAlyPL6 from human gut microbe *Bacteroides clarus*. Biochem Biophys Res Commun. 2021;547:111-117.
6. Zhang X, Qu Q, Yang A, Wang J, Cheng W, Deng Y, *et al*. Chitosan enhanced the stability and antibiofilm activity of self-propelled Prussian blue micromotor. Carbohydr Polym. 2023;299:120134.
7. Arroyo BJ, Bezerra AC, Oliveira LL, Arroyo SJ, de Melo EA, Santos AMP, *et al*. Antimicrobial active edible coating of alginate and chitosan add ZnO nanoparticles applied in guavas (*Psidium guajava* L.). Food Chem. 2020;309:125566.
8. Makaremi M, Yousefi H, Cavallaro G, Lazzara G, Goh CBS, Lee SM, *et al*. Safely dissolvable and healable active packaging films based on alginate and pectin. Polymers. 2019;11(10):1594.
9. Yang S, Gu Y, Qu Q, Zhu G, Liu G, Battaglia VS, *et al*. Engineered Si@ alginate microcapsule-graphite composite electrode for next generation high-performance lithium-ion batteries. Electrochim Acta. 2018;270:480-489.
10. Elwakeel KZ, Ahmed MM, Akhdhar A, Sulaiman MG, Khan ZA. Recent advances in alginate-based adsorbents for heavy metal retention from water: a review. Desalin Water Treat. 2022;272:50-74.
11. Fila D, Hubicki Z, Kołodyńska D. Fabrication, characterization and evaluation of an *alginate-lignin* composite for rare-earth elements recovery. Materials. 2022;15(3):944.
12. Finotelli PV, Da Silva D, Sola-Penna M, Rossi AM, Farina M, Andrade LR, *et al*. Microcapsules of alginate/chitosan containing magnetic nanoparticles for controlled release of insulin. Colloids and Surfaces B: Biointerfaces. 2010;81(1):206-211.
13. Rinaudo M. Main properties and current applications of some polysaccharides as biomaterials. Polymer international. 2008;57(3):397-430.
14. Alheety MA, Raoof A, Al-Jibori SA, Karadağ A, Khaleel AI, Akbaş H, *et al*. Eco-friendly C60-SESMP-Fe3O4 inorganic magnetizable nanocomposite as high-performance adsorbent for magnetic removal of arsenic from crude oil and water samples. Materials Chemistry and Physics. 2019;231:292-300.
15. Raoof Mahmood A, Alheety MA, Asker MM, Zyaad Tareq A, Karadağ A. Saccharine based carbonyl multi-walled carbon nanotubes: Novel modification, characterization and its ability for removing Cd (II) and Cu (II) from soil and environmental water samples. Journal of Physics: Conference Series. 2019 Sep;1294(5):052003.
16. Shakiba M, Kakoei A, Jafari I, Rezvani Ghomi E, Kalaee M, Zarei D, *et al*. Kinetic modeling and degradation study of liquid polysulfide resin-clay nanocomposite. Molecules. 2021;26(3):635.
17. El-Naggar ME, Wassel AR, Shoueir K. Visible-light driven photocatalytic effectiveness for solid-state synthesis of ZnO/natural clay/TiO2 nanoarchitectures towards complete decolorization of methylene blue from aqueous solution. Environmental Nanotechnology, Monitoring & Management. 2021;15:100425.
18. Pitaloka NF, Sriwijayanti A, Anisa S, Wijayanti IDA. Utilization Of Sugarcane Bagasse Cellulose-Clay Nanocomposite As A Biodegradable And Antibacterial Packaging Material To Extend The Food's Shelf Life. Khazanah: Jurnal Mahasiswa, 2020, 12(2).
19. Hariram M, Ganesan V, Muthuramkumar S, Vivekanandhan S. Functionalization of kaolin clay with silver nanoparticles by *Murraya koenigii* fruit extract-mediated bioreduction process for antimicrobial applications. Journal of the Australian Ceramic Society. 2021;57:505-513.
20. Châu NH, Thúy NT, Hiền ĐT, Mai HT, Quang NV, Long PH, *et al*. Study on antifungal activity of silver/bentonite nanomaterials on soybean phytopathogenic fungi. Vietnam Journal of Biotechnology. 2017;15(2):349-357.
21. Zhao Q, Fu L, Jiang D, Ouyang J, Hu Y, Yang H, *et al*. Nanoclay-modulated oxygen vacancies of metal oxide. Communications Chemistry. 2019;2(1):11.
22. Feng Y, Wang Y, Wang Y, Liu S, Jiang J, Cao C, *et al*. Simple fabrication of easy handling millimeter-sized porous attapulgite/polymer beads for heavy metal removal. Journal of colloid and interface science. 2017;502:52-58.
23. Wei X, Cheng F, Yao Y, Yi X, Wei B, Li H, *et al*. Facile synthesis of a carbon dots and silver nanoparticles (CDs/AgNPs) composite for antibacterial application. RSC advances. 2021;11(30):18417-18422.
24. Torabian F, Akhavan Rezayat A, Ghasemi Nour M, Ghorbanzadeh A, Najafi S, Sahebkar A, *et al*. Administration of silver nanoparticles in diabetes mellitus: a systematic review and meta-analysis on animal studies. Biological Trace Element Research. 2022;200(4):1699-1709.
25. Song Y, Yang F, Mu B, Kang Y, Hui A, Wang A, *et al*. Phyto-mediated synthesis of Ag nanoparticles/attapulgite nanocomposites using olive leaf extract: Characterization, antibacterial activities and cytotoxicity. Inorganic Chemistry Communications. 2023;151:110543.
26. Nath D, Banerjee P. Green nanotechnology-a new hope for medical biology. Environmental toxicology and pharmacology. 2013;36(3):997-1014.
27. Akhtar MS, Panwar J, Yun YS. Biogenic synthesis of metallic nanoparticles by plant extracts. ACS Sustainable Chemistry & Engineering. 2013;1(6):591-602.
28. Baker S, Rakshith D, Kavitha KS, Santosh P, Kavitha HU, Rao Y, *et al*. Plants: Emerging as nanofactories towards facile route in synthesis of nanoparticles. Bio. Impacts: BI. 2013;3(3):111.
29. Rai M, Yadav A. Plants as potential synthesiser of precious metal nanoparticles: progress and prospects. IET nanobiotechnology. 2013;7(3):117-124.

30. Yousaf H, Mehmood A, Ahmad KS, Raffi M. Green synthesis of silver nanoparticles and their applications as an alternative antibacterial and antioxidant agents. Materials Science and Engineering: C. 2020;112:110901.
31. Alharbi NS, Alsubhi NS, Felimban AI. Green synthesis of silver nanoparticles using medicinal plants: Characterization and application. Journal of Radiation Research and Applied Sciences. 2022;15(3):109-124.
32. Li Z, Yu D, Wangbao G, Guangjun W, Ermeng Y, Jun X, *et al*. Aquatic ecotoxicology and water quality criteria of three organotin compounds: A review. Nat Environ Pollut. Technol. 2019;18:217-224.
33. Duan B, Wang M, Zhou WY, Cheung WL, Li ZY, Lu WW, *et al*. Three-dimensional nanocomposite scaffolds fabricated via selective laser sintering for bone tissue engineering. Acta biomaterialia. 2010;6(12):4495-4505.
34. Mahto TK, Pandey SC, Chandra S, Kumar A, Kumar Sahu S. Hydroxyapatite conjugated graphene oxide nanocomposite: A new sight for significant applications in adsorption. RSC advances. 2015;5(117):96313-96322.
35. Simon FG, Biermann V, Peplinski B. Uranium removal from groundwater using hydroxyapatite. Applied Geochemistry. 2008;23(8):2137-2145.
36. Ibrahim M, Labaki M, Giraudon JM, Lamonier JF. Hydroxyapatite, a multifunctional material for air, water and soil pollution control: A review. Journal of hazardous materials. 2020;383:121139.
37. Pai S, Kini SM, Selvaraj R, Pugazhendhi A. A review on the synthesis of hydroxyapatite, its composites and adsorptive removal of pollutants from wastewater. Journal of Water Process Engineering. 2020;38:101574.
38. Wang L, Sheng J. Preparation and properties of polypropylene/org-attapulgite nanocomposites. Polymer. 2005;46(16):6243-6249.
39. Elbahnasawy MA, Shehabeldine AM, Khattab AM, Amin BH, Hashem AH. Green biosynthesis of silver nanoparticles using novel endophytic *Rothia endophytica*: Characterization and anticandidal activity. Journal of Drug Delivery Science and Technology. 2021;62:102401.
40. Dong Y, Dong W, Cao Y, Han Z, Ding Z. Preparation and catalytic activity of Fe alginate gel beads for oxidative degradation of azo dyes under visible light irradiation. Catalysis Today. 2011;175(1):346-355.